

CONTROL OF LASER RADIATION PARAMETERS

https://doi.org/10.1070/QEL16726

Generation regimes of an Nd:YAG laser with mode locking by a travelling-wave acousto-optic modulator and spherical mirror

A.V. Gribanov, V.I. Donin, D.V. Yakovin

Abstract. **The lasing regimes of a diode-pumped Nd:YAG laser with mode locking by a spherical mirror and a travelling-wave acousto-optic modulator (SMAOM method) are investigated. The lasing dynamics at mode spacing detuning from the doubled operating modulator frequency and with a change in the diffraction modulator efficiency is studied. The results of measuring the pulse duration and the frequency spectrum of output radiation are presented.**

Keywords: *Nd:YAG laser, diode pumping, Q-switching, mode locking, relaxation oscillations.*

1. Introduction

A new method was proposed in [1–4], which makes it possible to provide simultaneously mode locking and Q-switching [Q-switched mode locking (QML)] in solid-state lasers. The QML regime was implemented using a combination of a cavity spherical mirror and a travelling-wave acousto-optic modulator (AOM) (the SMAOM method). In those studies, Q-switching was provided by switching off periodically a sound wave. It was found in [5] that the QML regime may also arise without switching off the sound wave; Q-switching was performed at the laser relaxation-oscillation frequency. This regime, referred to as autoQML, was observed when the laser mode spacing was equal to the doubled frequency of the modulator travelling sound wave. This regime was previously implemented in solid-state lasers with a standing-wave AOM [6–8]; however, it arose only when the mode spacing was detuned from the modulator sound wave frequency. It was noted in [6–8] that this generation regime has a drawback: increase in the individual pulse duration in a train (in comparison with the case of exact correspondence between the mode spacing and sound frequency). Nanii et al. [9] applied the theory developed in [10, 11] to analyse the autoQML regime with a travelling-wave AOM and showed that the diffraction coupling coefficient k_d (AOM diffraction efficiency) can be used as a control parameter to drive dynamic generation regimes.

In this paper, we report the results of studying the generation dynamics of an Nd:YAG laser with SMAOM in dependence of the AOM diffraction efficiency and detuning of the laser mode spacing from the doubled frequency of modulator travelling sound wave. The output-pulse duration in different lasing regimes and at different polarisations of radiation in the cavity was measured by the autocorrelation method. In addition, the output frequency spectrum was recorded.

A.V. Gribanov, V.I. Donin, D.V. Yakovin Institute of Automation and Electrometry, Siberian Branch, Russian Academy of Sciences, prosp. Akad. Koptyuga 1, 630090 Novosibirsk, Russia; e-mail: donin@iae.nsk.su

Received 11 May 2018
Kvantovaya Elektronika **48** (8) 699–702 (2018)
Translated by Yu.P. Sin'kov

2. Schematic of the experiment

A schematic of a laser with a four-mirror Z-shaped cavity is shown in Fig. 1. The active element is an Nd:YAG crystal 2 mm in diameter and 63 mm in length, with diode side pumping at $\lambda = 808$ nm. Mirror M2 is flat; the curvature radii of spherical mirrors M1, M3, and M4 are, respectively, 300, 200, and 150 mm. The reflectance of dense mirrors M2–M4 at the operating wavelength (1064 nm) exceeds 99.5%. The output mirror transmittance is 14% at $\lambda = 1064$ nm. Fused silica Brewster plates can be rotated by 90° with respect to the cavity optical axis, providing a desired polarisation of radiation: either perpendicular ($\perp$) or parallel ($\parallel$) to the horizontal plane. The optical cavity length is $L \sim 150$ cm. An acousto-optic modulator with antireflective end faces (model MZ-322) is located near terminal spherical mirror M1 and makes a Bragg angle with the optical cavity axis. The optical path length between mirror M1 and modulator centre is equal to the curvature radius of this mirror. Operating frequency $f = 50049.6$ kHz, equal to half the laser mode spacing ($c/2L = 2f$), was applied to the AOM piezoelectric transducer.

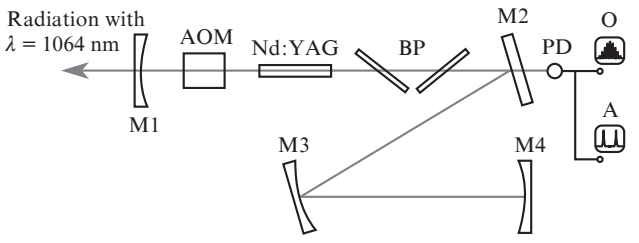

Figure 1. Schematic of the laser system:
(M1–M4) cavity mirrors; (BP) Brewster plates; (PD) avalanche photodiode; (O) oscilloscope; (A) spectrum analyser.

The radiation passing through dense mirror M2 was recorded by an LFD-2 avalanche photodiode, whose output signal was directed to an oscilloscope and an SF 300 spectrum analyser (Rohde&Schwarz).

3. Results and discussion

Initially we performed experiments with invariable AOM diffraction efficiency ($k_d = 2.5\%$). The cavity length was changed;

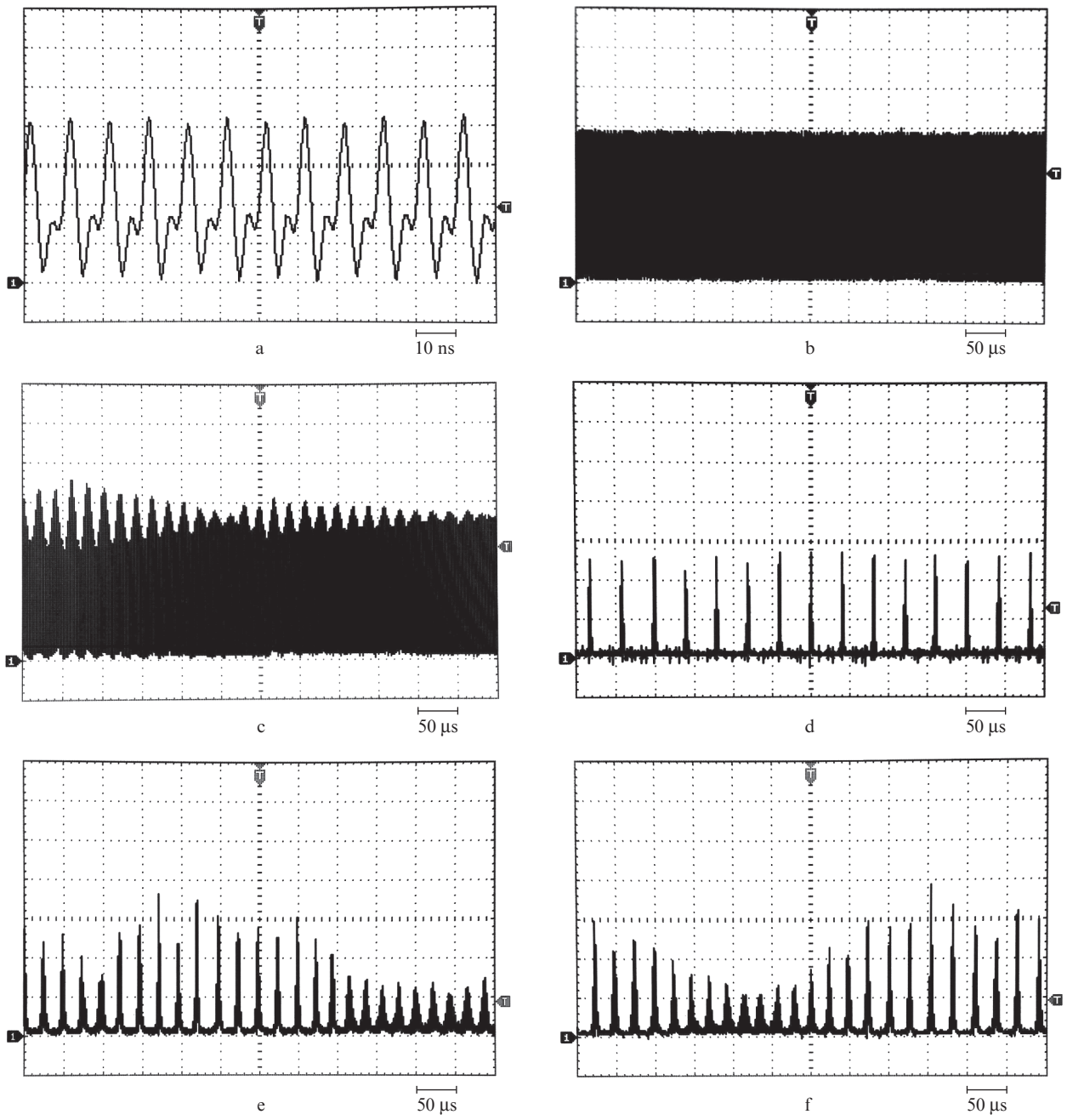

Figure 2. Oscillograms of the laser output at ΔL = (a, b) 0, (c) ±3, (d) ±70, (e) –600, and (f) 400 μm. The minus sign indicates a decrease in the cavity length.

i.e., a detuning of laser mode spacing from frequency $2f$ was introduced. CW mode locking (CWML), presented in Figs 2a and 2b, was observed within the cavity length detuning $\Delta L \approx \pm 2$ μm, which corresponds to a frequency detuning of $\Delta\nu \approx \pm 130$ Hz. A gradual increase in detuning led to occurrence of pulsations (Fig. 2c), which were gradually transformed into autoQML lasing (Fig. 2d) at $\Delta L = \pm 70$ μm ($\Delta\nu \approx \pm 4.7$ kHz). This regime remained stable up to detunings $\Delta L \approx -600$ μm ($\Delta\nu \approx -40$ kHz) and $\Delta L \approx 400$ μm ($\Delta\nu \approx$ 27 kHz), at which the regime began to lose stability (Figs. 2e, 2f). With an increase in detuning, the pulse train frequency changed from 25 kHz at $\Delta L = \pm 70$ μm to 40 kHz at $\Delta L = -600$ μm and $\Delta L = 400$ μm. It should be emphasised that complete mode locking was observed in the entire detuning range within a train.

Our experiments showed that, when the cavity length is tuned exactly ($\Delta L = 0$), the lasing regime depends on the coefficient k_d. CW mode locking was observed at an acoustic signal power of ~0.2 W and corresponding diffraction efficiency $k_d = 2.5\%$. An increase in acoustic power led to the occurrence of pulsations, similar to those shown in Fig. 2c. Stable autoQML was observed when the acoustic signal power reached approximately 0.5 W ($k_d = 10\%$). A further increase in the acoustic power disturbed autoQML: pulsations became irregular, as in Figs 2e and 2f. This lasing regime retained up to its disappearance at an acoustic signal power of ~1.32 W ($k_d = 27\%$). QML lasing was implemented at the same power (by switching off periodically a 2-kHz acoustic signal).

Figure 3 shows the laser output frequency spectrum in the vicinity of resonance frequency $c/2L$ in the CWML and auto-

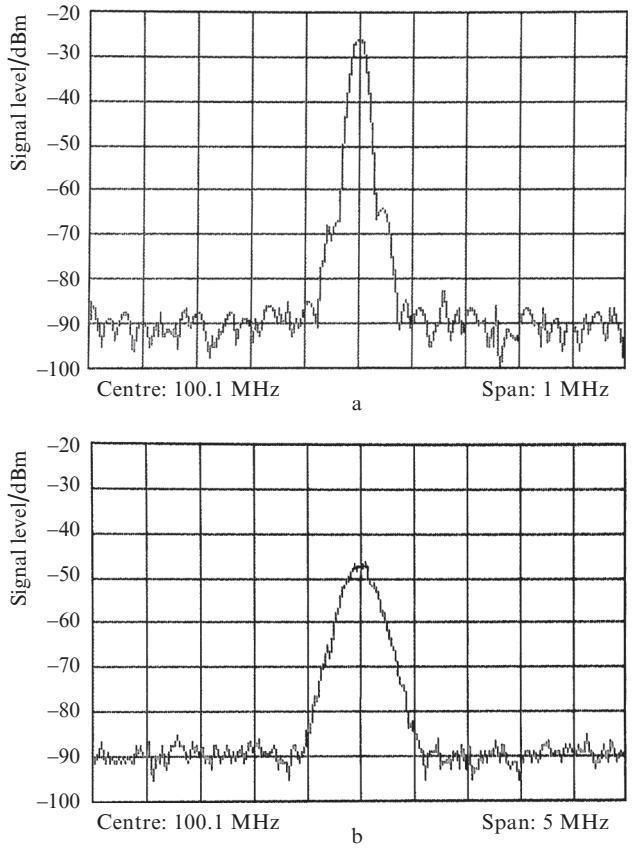

Figure 3. Fragment of a lasing spectrum in the spectrum analyser screen at $\Delta L = 0$: (a) CWML regime (the scale-division value on the abscissa axis is 100 kHz) and (b) autoQML regime (the scale-division value on the abscissa axis is 500 kHz).

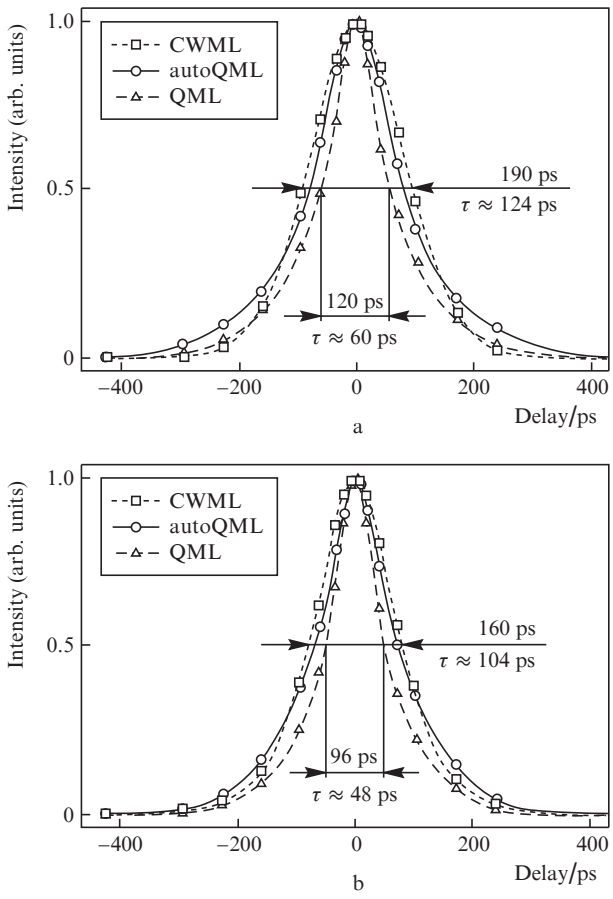

Figure 4. Pulse autocorrelation functions at $\Delta L = 0$ in the CWML, autoQML, and QML lasing regimes for the (a) $\perp$ and (b) $\parallel$ polarisations of radiation in cavity.

QML regimes at $\Delta L = 0$. In Fig. 3a, one can see weak side components at the relaxation frequency. The signal-to-noise ratio was ~60 and ~40 dB in the CWML and autoQML regimes, respectively. The frequency spectrum in the QML regime was previously studied by us in [12].

The output pulse duration was measured by an optical correlator with second-harmonic generation in a nonlinear crystal according to the noncollinear scheme. Measurements were performed for $\perp$ and $\parallel$ polarisations in a cavity with exactly tuned length ($\Delta L = 0$). When rotating Brewster plates, the AOM was also rotated by 90°. The light polarisation and sound wave propagation directions in the AOM were orthogonal.

The results of measuring the pulse duration τ are presented in Fig. 4. The shape of the pulse autocorrelation function in the CWML regime is close to that of the function sech^2. In this case, the pulse duration was 104 and 124 ps for the $\parallel$ and $\perp$ polarisations, respectively. In the autoQML regime, the shape of the autocorrelation function changed: its edge remained wide, whereas the central part narrowed. This effect is even more pronounced in the QML regime, where the shape of the autocorrelation function was similar to that for a single-sided exponential pulse. On the assumption of exponential shape of pulses, their duration in the autoQML regime is 70 for the $\parallel$ polarisation and 80 ps for the $\perp$ polarisation. In the QML regime, their duration is 48 and 60 ps for the $\parallel$ and $\perp$ polarisations, respectively. It should be noted that this autocorrelation function is the result of averaging of a large number of pulses (~10^8 in the autoQML regime and ~10^6 in the QML regime), because each measurement took about 1 min. The pulse duration may change from train to train; in addition, the number of pulses per axial period may also change [12]. The case of variable pulse duration was considered in [13]; the corresponding autocorrelation functions took an exponential shape. Therefore, within this study, it appears rather difficult to determine the exact pulse duration in the autoQML and QML regimes from the autocorrelation functions. Note that the pulse duration in the autoQML and QML regimes was previously measured by a streak camera [5, 12].

Figure 5 shows the autocorrelation function of pulses in the autoQML regime at $k_d = 2.5\%$ and $\Delta L \approx 100$ μm. It can be seen that cavity length detuning led to a significant broadening of the autocorrelation function edges in comparison with the case of autoQML at $k_d = 10\%$ and $\Delta L = 0$. This circumstance may indicate occurrence of several pulses per axial laser period, as was observed previously in [5]. A similar broadening of the autocorrelation function under detuning conditions occurred also in the QML regime.

The obtained difference in the pulse durations at different polarisations of light in the cavity can be explained by the light beam astigmatism. According to the cavity matrix calculation, due to the astigmatism, the beam diameter at the AOM centre in the horizontal plane is wider by a factor of 1.2 than in the perpendicular plane. To check the influence of

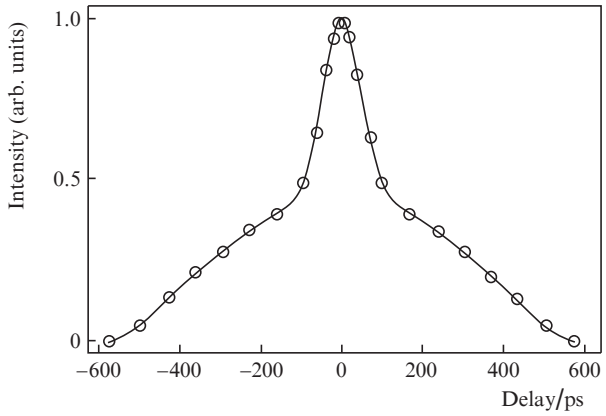

Figure 5. Autocorrelation function in the autoQML regime at $\Delta L \approx 100$ μm and $k_d = 2.5\%$.

astigmatism, we designed a cavity without astigmatism. In this case, the pulse duration was the same for the || and ⊥ polarisations.

The average output laser power (P_{out}) in the CWML regime was 1 W. When the autoQML regime was provided by detuning the cavity length, we did not observe any decrease in the output power. When the laser operated in the autoQML regime implemented by increasing k_d, the output power decreased to 620 mW because of the increased diffraction loss. In the QML regime, $P_{out} = 580$ mW. The decrease in the average power in the QML regime at low Q-factor modulation frequencies reflects the known tendency (see, e.g., [14]) and is due to the increased transfer of useful excitation power to spontaneous emission.

4. Conclusions

We should note that the SMAOM method, proposed to increase the peak pulse power, provides lasing not only in QML but also in autoQML and CWML regimes. The shortest (~50 ps) pulses were obtained under the QML conditions. The autoQML regime can be implemented by either changing the AOM diffraction efficiency or detuning the laser mode spacing from the doubled frequency of modulator travelling sound wave ($\Delta\nu \approx 5-30$ kHz). The shape of the pulse autocorrelation function changes when passing from CWML to autoQML and QML regimes. The autocorrelation function shape is distorted most strongly when the laser mode spacing is detuned from the doubled frequency of modulator travelling sound wave. This is explained by the occurrence of several pulses per axial laser period. Note also that the output pulse duration depends on the light beam astigmatism (shorter pulses were generated in the AOM sound wave propagation direction at a smaller beam diameter).

References

1. Donin V.I., Yakovin D.V., Gribanov A.V. *Quantum Electron.*, **42**, 107 (2012) [*Kvantovaya Elektron.*, **42**, 107 (2012)].
2. Donin V.I., Yakovin D.V., Gribanov A.V. *Opt. Lett.*, **37**, 338 (2012).
3. Donin V.I., Yakovin D.V., Gribanov A.V. RF Patent No. 2478242 (March 27, 2013).
4. Donin V.I., Yakovin D.V., Gribanov A.V., Yakovin M.D. *Opt. Zh.*, **85**, 8 (2018).
5. Donin V.I., Yakovin D.V., Gribanov A.V. *JETP Lett.*, **101**, 783 (2015) [*Pis'ma Zh. Eksp. Teor. Fiz.*, **101**, 881 (2015)].
6. Eichler H.J. *Opt. Commun.*, **56**, 351 (1986).
7. Maciel A.C., Maly P., Ryan J.F. *Opt. Commun.*, **61**, 125 (1987).
8. Kean P., Smith K., Sibbett W. *Opt. Commun.*, **61**, 129 (1987).
9. Nanii O.E., et al. *Quantum Electron.*, **47**, 1000 (2017) [*Kvantovaya Elektron.*, **47**, 1000 (2017)].
10. McDuff O., Harris S. *IEEE J. Quantum Electron.*, **3**, 101 (1967).
11. Hjelme D.R., Mickelson A.R. *IEEE J. Quantum Electron.*, **28**, 1594 (1992).
12. Donin V.I., Yakovin D.V., Gribanov A.V. *Quantum Electron.*, **45**, 1117 (2015) [*Kvantovaya Elektron.*, **45**, 1117 (2015)].
13. Van Stryland E.W. *Opt. Commun.*, **31**, 93 (1979).
14. Donin V.I., Nikonov A.V., Yakovin D.V. *Quantum Electron.*, **34**, 930 (2004) [*Kvantovaya Elektron.*, **34**, 930 (2004)].